

Local structure determination for low-coverage CO on Ni(111)

This article has been downloaded from IOPscience. Please scroll down to see the full text article.

1996 J. Phys.: Condens. Matter 8 1367

(<http://iopscience.iop.org/0953-8984/8/10/009>)

View [the table of contents for this issue](#), or go to the [journal homepage](#) for more

Download details:

IP Address: 171.66.16.208

The article was downloaded on 13/05/2010 at 16:21

Please note that [terms and conditions apply](#).

Local structure determination for low-coverage CO on Ni(111)

R Davis[†], D P Woodruff[†], Ph Hofmann[‡], O Schaff[‡], V Fernandez[‡],
K-M Schindler[‡], V Fritzsche^{‡§} and A M Bradshaw[‡]

[†] Physics Department, University of Warwick, Coventry CV4 7AL, UK

[‡] Fritz-Haber-Institut der Max-Planck-Gesellschaft, Faradayweg 4–6, 14195 Berlin (Dahlem), Germany

Received 30 November 1995

Abstract. Scanned-energy-mode photoelectron diffraction has been used to determine the local adsorption structure of CO on Ni(111) at low temperature at a coverage of approximately 0.25 ML, corresponding to a nominal (2×2) phase. CO molecules are found to occupy the same two ('hcp' and 'fcc') inequivalent hollow sites as in the 0.5 ML $c(4 \times 2)$ -CO phase, and while the results do indicate a preference for the hcp hollow site directly above a second-layer Ni atom in the low-coverage state, this preference ($65 \pm 20\%$) is of marginal statistical significance. The similarity of this parameter in both the (2×2) and $c(4 \times 2)$ phases can only be reconciled by assuming significant local disorder. It does, however, indicate that the local binding energies at the two hollow sites are very similar and that the presence of both sites in the $c(4 \times 2)$ phase is not simply a consequence of near-neighbour adsorbate–adsorbate repulsion.

1. Introduction

The adsorption of CO on Ni surfaces is often regarded as one of the most archetypal of molecular adsorption systems studied in surface science and has been subjected to a large number of experimental and theoretical investigations. Despite this, recent photoelectron diffraction (PhD) [1, 2] and SEXAFS [3] (surface-extended x-ray absorption fine-structure) investigations have shown that the Ni(111) $c(4 \times 2)$ -CO phase, the best-known structural phase of CO on Ni(111), has a quite different local structure to that which had been previously widely supposed. In particular, vibrational spectroscopy had identified the C–O stretching frequency of this phase as occurring at about 1900 cm^{-1} , and the smooth increase in this frequency from lower coverages (assumed to be due to dynamic dipole coupling and other effects) from 1830 cm^{-1} had been interpreted as indicative of local bridge bonding of the adsorbed CO [4–13]. True quantitative structure determinations by PhD and SEXAFS, however, have shown that the $c(4 \times 2)$ -CO phase involves equal occupation of the two inequivalent hollow sites—the so-called 'hcp' and 'fcc' hollows corresponding to sites directly above Ni atoms in the second and third substrate layers, respectively (figure 1(a)). This conclusion has been further confirmed recently by a quantitative LEED (low-energy electron diffraction) study [14].

This 'double-hollow' structure is rather unusual. There have been many structural studies of atomic and molecular adsorption systems on fcc (111) surfaces which have

§ Present address: Institut für Theoretische Physik, Technische Universität Dresden, 01062 Dresden, Germany.

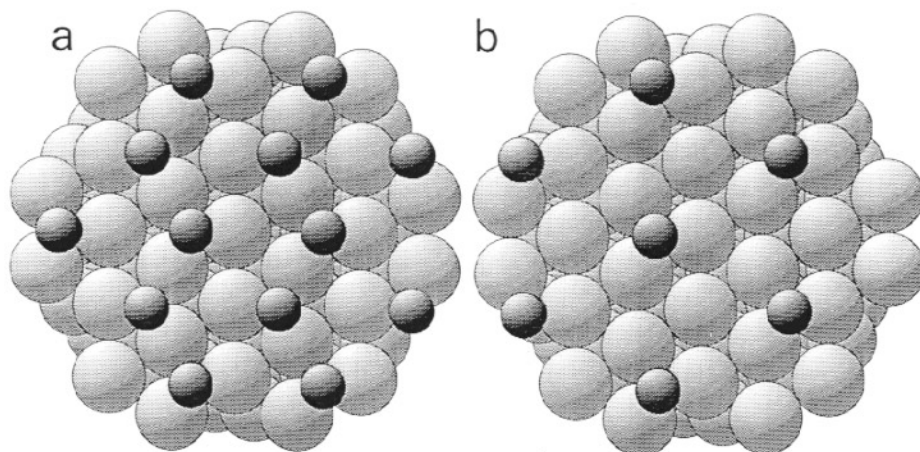


Figure 1. Plan views of hard-sphere models of: (a) the Ni(111)c(4 × 2)-CO structure as previously determined; and (b) a model of the Ni(111)(2 × 2)-CO structure based on occupation of 'hcp' hollow sites only.

concluded that hollow adsorption sites are occupied [15], but in almost [16] all cases the preferred site has been concluded to be the fcc hollow. The two hollow sites typically only differ in third or higher nearest neighbours, so one might expect that the difference in the binding energy of the two sites would be very small and that no such clear site preference would occur. On the other hand, most of these studies have been of long-range-ordered structures having only one adsorbate atom or molecule per unit mesh, a situation which formally implies only a single adsorption site, and in which the cooperative effect of the long-range order may greatly enhance the favourability of one site over another, relative to that experienced by an isolated adsorbate. Indeed, there is at least one example (iodine adsorption on Ag(111) [17, 18]) for which early photoelectron diffraction experiments have been interpreted as indicating that whilst the $(\sqrt{3} \times \sqrt{3})R30^\circ$ ordered phase (having one adsorbate atom per unit mesh) involves occupation of fcc hollow sites alone, the data from the lower-coverage disordered phase can be reconciled with approximately equal occupation of the two hollows. Similarly, there have been qualitative arguments to suggest that in the case of oxygen adsorption on Ni(111), for which the ordered phases again have O atoms only in the fcc hollows [19, 20], both hollows may be occupied in intermediate phase regions involving domain wall boundaries between islands of long-range order [21].

The double-hollow structure of the Ni(111)c(4 × 2)-CO phase, having *two* adsorbed molecules per unit mesh, might therefore be seen as entirely consistent with a pattern of behaviour in which the preference for the occupation of a single hollow site is a consequence only of the constraints of specific long-range order, and a very marginal difference in binding energy at the two sites for isolated molecules. On the other hand, a further feature of this structural phase is that the CO–CO nearest-neighbour distance is rather short (2.88 Å), and in particular is shorter than that which would be involved in a perfectly regular CO submesh (3.29 Å), but not as short as that required of a structure which involved only occupation of a single hollow site (2.49 Å). An alternative view is thus that the occupation of the two different hollow sites is a consequence of a nearest-neighbour adsorbate–adsorbate repulsion which is greater than the difference of the local adsorbate–substrate binding energy of the

two hollow sites, and that at a lower coverage only a single hollow site would be occupied. In the light of these quite different viewpoints, it is of interest to try to establish the local bonding geometry of CO at a significantly lower coverage than of 0.5 ML associated with the ordered $c(4 \times 2)$ phase.

Here we report on the results of such an investigation. We have applied the technique of scanned-energy-mode photoelectron diffraction determination [22, 23] to determine the local adsorption structure of CO on Ni(111) at low temperature at a nominal coverage of 0.20 ML, which we have found to show a previously unreported ordered (2×2) LEED pattern. In view of the fact that this implies a structure having one CO molecule per unit mesh, we would expect to have only one local site occupied. In fact we find that although the best-fit structure is one in which the majority of the CO molecules occupy the hcp hollow site, there remain a substantial fraction of molecules in the fcc hollow, and indeed the deviation from equal occupation of the two sites is not found to be statistically significant. We discuss this observation also in the context of recent studies of the local CO adsorption site on Ni(111) in surface phases involving CO/O [24] and CO/K [25, 26] coadsorption.

2. Experimental details and results

The experiments were performed at the BESSY synchrotron radiation facility in Berlin, taking radiation from the high-energy toroidal grating monochromator (HETGM) of the Fritz Haber Institute [27]. The surface science experimental chamber is fitted with a 152 mm mean radius spherical sector analyser fitted with three-channel parallel detection (VG Scientific), installed at a fixed angle of 60° to the incident soft x-ray beam in the plane of polarization. The Ni(111) sample was prepared by the usual combination of x-ray Laue alignment, spark machining, mechanical polishing, and *in situ* argon-ion bombardment and annealing cycles until a clean well-ordered surface was obtained as judged by soft-x-ray photoelectron spectroscopy (SXPS) and low-energy electron diffraction (LEED). The sample was dosed at a temperature of 115 K with approximately 2×10^{-6} mbar s of CO which yielded a clearly visible (2×2) LEED pattern and an average coverage estimated from comparison of the SXPS spectrum with that of the $c(4 \times 2)$ -CO phase to be approximately 0.20 ML. This coverage estimate is probably accurate to no better than $\pm 25\%$ bearing in mind the effects of photoelectron diffraction on the measured SXPS signals and the range of coverages which may correspond to the calibration reference of the $c(4 \times 2)$ phase. Somewhat surprisingly, there appears to be no report in the literature of a (2×2) -CO phase on Ni(111). On the other hand, despite the large number of previous investigations of the Ni(111)/CO surface interaction, there are no really exhaustive studies of the range of coverage and temperature corresponding to the different ordered phases. Most of the earlier studies [28–30] (and indeed many of the later ones [32, 6, 7, 33]), which do report the ordered LEED patterns seen, were conducted only close to room temperature. In some cases, higher coverages were achieved at room temperature by investigating the LEED pattern while the surface was held in a partial pressure of CO, and there was evidence for electron beam damage effects [29, 30]. The main structures reported are $(\sqrt{3} \times \sqrt{3})R30^\circ$, $c(4 \times 2)$ and $(\sqrt{7}/2 \times \sqrt{7}/2)R19^\circ$. The nominal coverages now generally agreed for these structures are 0.33 ML, 0.5 ML and 0.57 ML, although early work proposed a coverage of only 0.25 ML for the $c(4 \times 2)$ phase [32]. Careful reading of these papers indicates that most observations of the $(\sqrt{3} \times \sqrt{3})R30^\circ$ phase refer to poor order or split-spots [31, 5, 33]. The phase with the highest coverage among these three is seen at room temperature only under an excess pressure of CO, but is stable in UHV at low temperatures. Studies conducted at

low temperatures (in the range 90–200 K) [31, 5, 7, 12] reported no new LEED structures, but in general they either concentrated on specific higher-coverage phases, or used a high-coverage LEED structure as a coverage calibration. Following the initial observation of the (2×2) phase in our PhD study at BESSY, we have extended the characterization of the LEED structures for CO on Ni(111) in a laboratory-based chamber at Warwick (using a different crystal). We found that it was possible to reproduce the (2×2) phase in addition to all the phases for which there are clear previous reports; consistent with these earlier publications, no sharp pure $(\sqrt{3} \times \sqrt{3})R30^\circ$ pattern was seen. During the course of this LEED characterization, however, we found that the CO-covered surface is very susceptible to electron beam damage, so the full range of structures could only be obtained in a series of experiments in which the surface was re-cleaned after each CO exposure. We also found that the (2×2) phase was only seen at low temperatures, and that annealing to higher temperature produced a $c(4 \times 2)$ LEED pattern. It is not clear whether this is due to islanding (implying *attractive* interactions) or whether the (2×2) phase actually involves some disorder in a latent $c(4 \times 2)$ pattern. We will return to this point later.

Scanned-energy-mode photoelectron diffraction [22, 23] measurements were made from the C 1s core level in a number of different emission geometries according to the methods which we have described in more detail previously (e.g. [34, 2, 22, 23]). Briefly, short-range photoelectron energy distributions around these two peaks were recorded at a succession of photon energies to yield photoelectron kinetic energies in the range 80–420 eV. The peaks were then separated from the background and integrated to yield peak area versus kinetic energy spectra. These spectra were then converted to PhD modulation spectra with the aid of a smooth spline which was subtracted from, and then divided into the raw peak areas. One problem which always arises in C 1s PhD spectra (see, e.g., [2]) is obtaining a good subtraction of the C KVV Auger electron peak which the photoelectron peak passes through at kinetic energies in the 260–300 eV range. In the present data, for which the coverage of CO is relatively low yielding a poorer signal-to-background ratio, this subtraction proved particularly troublesome, so to avoid the possibility of trying to reproduce spurious artifacts with the theoretical calculations, these parts of the experimental PhD spectra were omitted.

3. Structure determination

The method of structure determination which we have developed for PhD spectra involves two stages. First an approximate structure is obtained by a direct inversion of the experimental spectra. Secondly, full multiple-scattering simulations are computed for a range of trial structures in the range of parameter space identified by the direct method, and a best fit is found with the aid of a normalized squared-deviation reliability factor or *R*-factor, and a succession of trial-and-error iterations.

In order to establish the basic adsorption site we first apply a direct inversion method to a set of experimental C 1s PhD spectra. We have developed two methods of this type. Both rely on the fact that when the experimental geometry is such as to place a near-neighbour substrate atom directly behind the emitter to produce a favoured 180° scattering event, this scatterer and its associated effective pathlength difference dominates the PhD spectrum and leads to a characteristic high-amplitude and long-energy-periodicity modulation. In the simplest method [35–37] one simply identifies this geometry from experimental spectra taken over a wide range of emission directions by taking Fourier transforms and looking for the largest-amplitude feature with a short effective scattering pathlength. This then defines the nearest-neighbour backscattering direction and thus the emitter site. A refinement of this approach is the ‘projection’ method which takes account of scattering phase shifts to

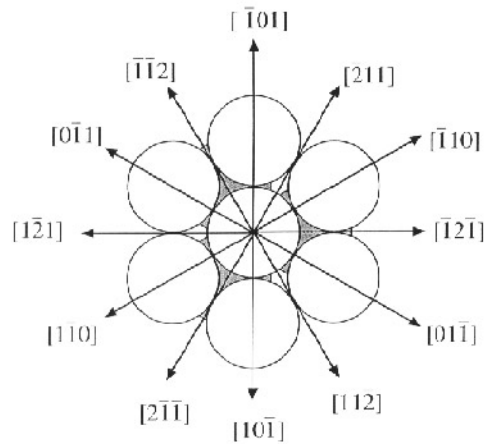


Figure 2. A schematic plan view of the top two layers of a Ni(111) surface defining the azimuthal directions as used in this paper. Note the equivalence of all $\langle 110 \rangle$ directions but the inequivalence of opposite $\langle 211 \rangle$ directions.

give a far more precise estimate of the emitter–scatterer distance as well as its direction, and which can be applied effectively to a significantly smaller data set [37–39]. In the present case, this projection method was applied to a subset of seven C 1s PhD spectra; these were normal-emission together with 20° and 40° polar emission angle measurements in each of the two inequivalent $\langle 211 \rangle$ azimuths and the $\langle 110 \rangle$ azimuth (see figure 2 for a definition of these azimuths). Figure 3 shows the result of this procedure; the method generates a three-dimensional map of a function which provides some measure of the probability of finding a backscatterer atom at a particular point in space, and the figure shows grey-scale maps of this function in two different two-dimensional cuts. In the upper panel is shown a cut perpendicular to the surface through the C emitter (at $(0, 0, 0)$) in a $\langle 211 \rangle$ azimuth; a single substrate atom feature is seen approximately 1.3 \AA below the emitter. In the lower (central) panel a cut parallel to the surface and 1.3 \AA below the emitter reveals that there are three features associated with Ni substrate scatterers, and the real-space directions of these atoms correspond to the nearest neighbours of the hcp hollow site alone (compare figures 2 and 3). Also shown for comparison is a similar projection method map of C 1s PhD data from the $c(4 \times 2)$ -CO phase on Ni(111). The cut parallel to the surface 1.35 \AA below the emitter in this case shows a set of six Ni-related features which are attributed to the three hcp site nearest neighbours, and the three fcc hollow site nearest neighbours rotated in azimuthal angle by 60° . Comparison of these two ‘images’ of the near-neighbour environments of the C atoms in the (2×2) -CO and $c(4 \times 2)$ -CO phases thus suggests that while the latter phase appears to involve equal occupation of the two hollow sites (as, indeed, we find in the full analysis of the data from this phase), the former may have CO molecules only in the hcp hollows. We should stress, however, that the projection method is specifically designed to identify the dominant near-neighbour scatterer locations only, so these results indicate only that the majority site may be the hcp hollow. A schematic diagram of a model of a (2×2) CO phase in which only hcp hollow sites are occupied is shown in figure 1(b) and may be compared with a similar view of the known structure of the $c(4 \times 2)$ phase in figure 1(a).

In order to define the structure more precisely, comparisons of full multiple-scattering calculations were then performed for a range of trial structures. For this purpose model

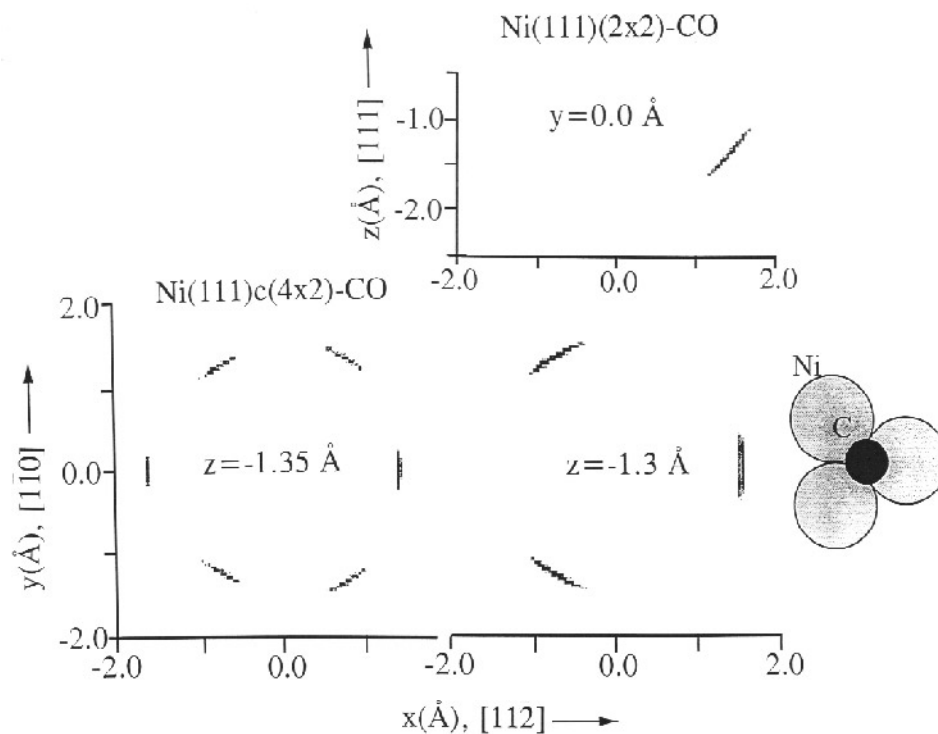


Figure 3. ‘Images’ of the C near-neighbour substrate scatterers for the Ni(111)(2 × 2)-CO phase (centre panels) obtained by application of the projection method to the C 1s PhD spectra, compared with similar data obtained from the Ni(111)c(4 × 2)-CO phase (lower left-hand panel) [1, 2]. Two cuts in three-dimensional space are shown. In the upper panel the cut is perpendicular to the surface passing through the C emitter located at (0, 0, 0); below is a cut parallel to the surface but 1.3 Å below the emitter for the (2 × 2) phase and 1.35 Å below the emitter for the c(4 × 2) phase. The three features shown in the (2 × 2) phase data can be attributed to nearest-neighbour Ni atoms for a C atom located in an hcp hollow site, directly above a second-layer Ni atom (see the schematic plan view). The six features seen in the c(4 × 2) phase data are attributed to the nearest Ni neighbours of both the hcp and fcc hollows.

Table 1. Optimized parameter values for the Ni(111)(2 × 2)-CO and Ni(111)c(4 × 2)-CO structures obtained by photoelectron diffraction.

Parameter	Structural phase		
	(2 × 2) (this work)	c(4 × 2) [1, 2]	c(4 × 2) [26]
z_{Chcp}	$1.26 \pm 0.04 \text{ \AA}$	$1.29 \pm 0.06 \text{ \AA}$	$1.28 \pm 0.04 \text{ \AA}$
z_{Cfcc}	$1.30 \pm 0.08 \text{ \AA}$	$1.30 \pm 0.08 \text{ \AA}$	$1.32 \pm 0.07 \text{ \AA}$
z_{12}	$2.10 \pm 0.06 \text{ \AA}$	$2.10 \pm 0.15 \text{ \AA}$	$2.04_{-0.04}^{+0.12} \text{ \AA}$
%hcp sites	64 ± 22	64 ± 27	65 ± 25

calculations were conducted using multiple-scattering calculations which take into account the role of energy and angular apertures in the experiment [40–42] and exploit a linear approximation scheme [43] to search more efficiently the necessary parameter space defined by a series of structural parameters. The quality of the fit between theory and experiment

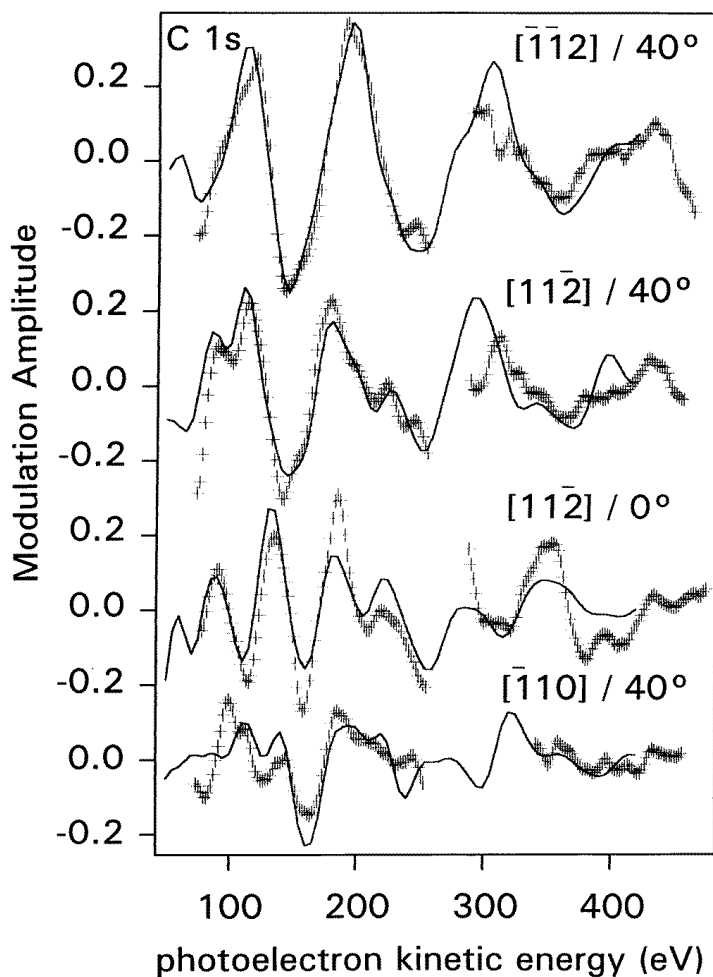


Figure 4. Experimental C 1s PhD spectra (+ symbols) used in the multiple-scattering structural optimization compared with the results of the calculations (full lines) for the best-fit structure as given in table 1.

was judged with the aid of an R -factor which is a normalized square deviation summed over all data points of PhD spectra recorded in several different emission directions [44]. The optimization was based on C 1s experimental PhD spectra recorded in the same four emission geometries as those used in the earlier determination of the $c(4 \times 2)$ structure [1, 2] (normal emission with incidence in the $\langle 110 \rangle$ azimuth and 40° polar angle emission in each of the three principal azimuths). Our general methodology for structure determination based on multiple-scattering analysis of PhD data is to choose a data set which covers a reasonable range of directions but includes, in particular, those PhD spectra which show the strongest modulations; these spectra are clearly the most reliable ones experimentally, but also typically provide the strongest sensitivity to near-neighbour bondlengths. In the present case, our desire to compare the structural solutions for the (2×2) and $c(4 \times 2)$ phases encourages us to choose the same emission directions for both analyses. The basic structural model for the (2×2) phase on which the present calculations concentrated was

one in which CO molecules are adsorbed (with the C–O axis perpendicular to the surface) in the hollow sites, but covered not only structures having only hcp hollow site occupation, but also incoherent averages of both hcp and fcc sites with varying relative concentrations. In this structural optimization process the parameters varied were the outermost C–Ni layer spacings at each site, z_{Chcp} and z_{Cfcc} , the Ni–Ni outermost layer spacing, z_{12} as well as the relative occupation of hcp and fcc hollow sites. The parameters obtained for the best-fit structure are summarized in table 1, and compared with the equivalent parameters obtained in the earlier published analysis of the $c(4 \times 2)$ phase [1, 2], together with the results of a recent reanalysis of photoelectron diffraction data from this latter phase including both C 1s and O 1s PhD spectra [26]. The best-fit calculations are compared with the experimental spectra in figure 4.

The detailed local structural parameters of the present analysis of the (2×2) -CO phase, i.e. the C–Ni and Ni–Ni layer spacings, agree with the values of both analyses of the $c(4 \times 2)$ phase to within the estimated error margins, a result which is not particularly surprising. What is surprising, however, is that the optimum fractional occupation of the hcp hollow sites is also unchanged; indeed, the values for the two phases are essentially identical despite the significant error estimate. In particular, the analyses of the two phases indicate a preference for hcp site occupation, but with error estimates which comfortably cover the 50% required of equal occupation, but which exclude the possibility of pure hcp site occupation.

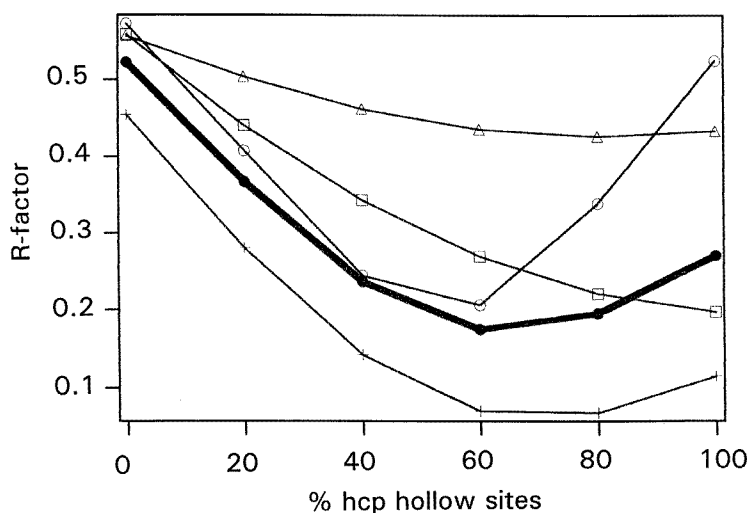


Figure 5. The dependence of the four-spectrum R -factor (the bold line), and of the individual single-spectrum R -factors (narrow lines), on the parameter defining the fractional occupation of hcp and fcc CO site occupation in the (2×2) -CO phase. The individual single-spectrum R -factors correspond to the following emission angles and azimuths: 40° in $[\bar{1}\bar{1}2]$ (+); 40° in $[11\bar{2}]$ (circles); 40° in $[\bar{1}10]$ (triangles); 0° in $[11\bar{2}]$ (squares).

Before addressing the general significance of these structural conclusions we should address a technical point concerning the methodology. In particular, while we have already highlighted the caveat that the projection method is only intended to indicate the probable majority adsorption site (which it has done in this case), the comparison of the projection ‘images’ shown in figure 3 for the (2×2) and $c(4 \times 2)$ structures does suggest that there

may be a qualitative difference between the two structures which is not borne out by the full simulations. Some insight into this problem is given by a study of the dependence of the R -factor on the parameter defining the fraction of hcp sites occupied. Figure 5 shows this dependence, not only for the four-spectrum R -factor covering the complete data set used in the analysis (see figure 4), but also the R -factors for each of these spectra separately. Because PhD spectra in principal backscattering directions can be dominated by specific single-atom scattering events, individual spectra can vary significantly in their sensitivity to certain structural parameters. Figure 5 shows not only a difference in the sensitivity of the different spectra to the hcp/fcc site occupation ratio, but also some differences in the optimum value. Thus, the lowest individual R -factor is obtained for the 40° $[\bar{1}\bar{1}\bar{2}]$ spectrum which, as may be seen from figure 2, corresponds to an emission direction which places a nearest-neighbour Ni atom directly behind a C emitter occupying the hcp hollow site. This spectrum clearly favours the hcp site (and is presumably dominated by the emitters occupying this site), although it is very insensitive to the hcp/fcc ratio in the range 1:1 to pure hcp. By contrast, the 40° $[11\bar{2}]$ spectrum, recorded in a backscattering geometry for an fcc site emitter, shows a stronger sensitivity to the site occupation but has its minimum close to a 1:1 ratio. The other off-normal spectrum, taken in the 40° $[\bar{1}\bar{1}0]$ direction, shows the worst R -factor, and varies rather little with occupation ratio except in the unfavoured pure fcc site region. Finally, the normal-emission spectrum actually shows its minimum value for the pure hcp site structure. The rather pronounced difference in the optimum value of the mixing parameter given by the normal-emission spectrum is rather unusual in our experience (and is not true, for example, for the data from the $c(4 \times 2)$ phase [26]). We should note, however, that the purpose of the multi-spectral R -factor, as in LEED, is precisely to provide a means of balancing slightly conflicting results of this kind, as well as to increase the confidence in the final solution. Moreover, careful consideration shows that these differences are not really statistically significant.

Our method of estimating the precision of structural conclusions follows the procedure devised for LEED by Pendry [45]; a variance in the R -factor is defined which depends on the magnitude of the R -factor at its minimum and the size of the associated data set. For the four-beam R -factor R_{\min} is 0.17 and the variance is estimated to be 0.04–0.05, so all structural parameter values leading to R -factors of less than 0.22 are believed to fall within one standard deviation, leading to an estimate of the hcp site occupation fraction of $64 \pm 22\%$. For the individual spectra the variance is typically larger both due to the smaller data set (four times smaller which doubles the variance) but also because the R_{\min} -values are worse for three of the four spectra. In the specific case of the normal-emission spectrum, the optimum value of the hcp fraction is clearly 100%, but the estimated error is 50%, so the result obtained with the multispectral R -factor in no way conflicts with this result. On the other hand, the tendency of the normal-emission data to favour a high hcp site occupation may account for the fact that the direct projection method also indicates a strong preference for this site; the projection method was applied to a data set which also included 20° emission data and so was more heavily weighted to near-normal emission. The moral, of course, is that such direct ‘images’ should be treated as indicative of the probable structure, and no substitute for a full analysis.

Of most significance here are the actual structural conclusions of this analysis; specifically that the optimum value of the hcp occupation parameter for the two different structural phases of CO, based on an equivalent data set, are essentially the same. Note too, that the reanalysis of the $c(4 \times 2)$ phase including additional (near-normal-emission) O 1s spectra, leads to no significant change in this parameter [26].

4. Discussion

The results of the present analysis present a dilemma. In a $c(4 \times 2)$ 0.5 ML phase, which contains two CO molecules per unit mesh, a structure comprising 50% hcp and 50% fcc sites is perfectly consistent with the long-range order of the LEED pattern, and with the hcp site occupation value of $64 \pm 27\%$ found in the PhD analysis [1, 2]. For a (2×2) 0.25 ML phase, each unit mesh can contain only one CO molecule, and if the structure has good long-range order, it cannot be reconciled with the same hcp fractional site occupation. The clear implication is that the surface that we have studied at the lower coverage does not comprise a single-domain long-range-ordered phase. Of course, the observation of a 'sharp' LEED pattern does not necessitate complete long-range order. LEED (like any diffraction method based on incident plane waves) specifically picks out the long-range-ordered part of the surface, and can lead to the observation of a 'good' LEED pattern (with little obvious visual increase in the background intensity) if as little as 10% of the surface shows good long-range order. LEED is also capable of picking out *average* order, although there may be significant local fluctuations in this order. There are therefore at least three possible solutions to the dilemma. One is that the (2×2) LEED pattern that we see represents only a small part of the surface, and that the remainder shows no good long-range order. The second possibility is that even the ordered parts show only average (2×2) periodicity, and that there are fluctuations of CO sites between fcc and hcp sites, which may be either static or dynamic. Both of these pictures are based on a mixture of long-range order and local disorder, and one might also envisage a situation which involves both components. A third and distinctly different possibility is that there are islands (domains) of ordered phase based on only hcp sites, and other islands based only on fcc sites. This model has been used to explain features of the Ni(111)/O phase diagram [21], but in a region in which anti-phase domain boundaries occur with implied adsorbate–adsorbate repulsive interactions rather than within coverage and temperature regions corresponding to simple commensurate overlayer LEED patterns.

Previous studies of CO adsorption on Ni(100) and Pt(100) provide an interesting comparison to the situation considered here. Most of these data are based on vibrational spectroscopy, and we have already seen in the CO/Ni(111) case that there are hazards in using such data for absolute adsorption site assignments, yet there are clear qualitative features for these other systems which should remain meaningful. Specifically, on Ni(100), CO is found to show two distinct C–O stretching frequencies which would typically be assigned to bridge and atop site adsorption [46–49]; even if we are cautious about these formal assignments, the coexistence of these two absorption bands is strongly indicative of two distinct states and probably two distinct sites. At low coverages (much less than 0.5 ML) the relative occupation of the two states has been found to be strongly temperature dependent in the range 80–310 K, and has been interpreted in terms of a small binding energy difference at the two sites. These results also show, however, that the 0.5 ML coverage state, which shows a $c(2 \times 2)$ LEED pattern, also shows a temperature-dependent mixture of the two states. One piece of evidence supporting the view that this mixture is associated with coexistent $c(2 \times 2)$ domains of the individual sites is the significant time delay required to establish equilibrium at different temperatures [49]. Similar results have been found for Pt(100) [50] and also interpreted in terms of coexisting ordered domains. The only true quantitative structural studies are early LEED analyses of Ni(100) $c(2 \times 2)$ -CO at room temperature [51, 52] which concluded that the CO molecules occupy atop sites (consistent with the implied majority phase seen in vibrational spectroscopy under these conditions), but this early work did not consider the possibility of mixed phases. Of course,

these results only provide further evidence that mixed sites can be occupied even when a LEED pattern is seen which implies a single adsorbed molecule per unit mesh and thus a single adsorption site within a long-range-ordered phase; they do not formally distinguish among the different structural models of the surface as a whole.

It is tempting, of course, to heighten the apparent dilemma of the local and long-range structural information in the present case by noting the almost exact correspondence of the optimum values of the hcp fractional site occupation for the two phases. At almost exactly 65% in both cases, one is forced to invoke major disorder in both phases. However, the error estimates are based on a formal application of variance estimates based on a statistically sound foundation [45], so we must accept that this exact coincidence is not formally significant. What our results do indicate, however, is that in Ni(111)/CO adsorption there does not appear to be a clear preference for one of the two hollow sites in the absence of strong adsorbate–adsorbate interactions, and that the mixed sites seen in the $c(4 \times 2)$ phase cannot be attributed to near-neighbour adsorbate repulsions. Rather, we must imply that the difference in binding energy for CO at the two sites is too small to produce a condensation into one site, at least at temperatures no lower than about 115 K.

In addition to the comparison of the (2×2) and $c(4 \times 2)$ CO adsorption phases on Ni(111), we should also remark on the results of some related PhD studies that we have performed on CO coadsorption on Ni(111). We have investigated two such phases. In the case of K coadsorption, we have studied the Ni(111) (2×2) -K/ n CO phase [25, 26] produced by forming a (2×2) -K surface phase and exposing this to a nominal saturation dose of CO. In this structure the K atoms retain their atop sites and the CO molecules, for which the coverage is approximately 0.5 ML implying a value of n of 2, occupy the two different hollow sites. The second phase studied is Ni(111) (2×2) -O/CO [24] formed by exposing a Ni(111) surface to oxygen to produce a (2×2) -O phase in which the O atoms occupy fcc hollow sites, and then saturating with CO, in this case achieving a coverage of CO of only about 0.25 ML. Again the CO occupies both hollow sites with a best-fit value of the fractional hcp site occupation of $70 \pm 35\%$. In this latter case the error estimates allows the possibility of pure hcp site occupation, yet the most probable solution remains one in which there is some random element of fcc or hcp site occupation for the CO molecules within the ordered matrix of the (2×2) -O structure. While the overall CO–substrate desorption energy is changed in these coadsorption systems relative to that for the pure CO layer, these results again indicate little site preference between the two hollow sites for the CO molecules.

One final discussion point concerns the possible generality of the conclusions. We have already commented on the parallels with the Ni(100)/CO and Pt(100)/CO systems as judged by vibrational spectroscopy fingerprinting, but there is almost no true quantitative structural information for other adsorption systems concerning changes of adsorption site with coverage, and particularly the possibility of changes in relative occupation of two or more sites. Most true structural studies so far have been based on surfaces showing good LEED patterns taken to imply single adsorption sites, and only single adsorption sites have been tested. Even in the few structural studies of disordered systems, this has commonly been an implicit assumption. In the few cases in which mixed (fcc and hcp hollow) sites have been deduced, such as the LEED study of the Ni(111) $c(4 \times 2)$ -CO phase [14] and the early photoelectron diffraction study of I on Ag(111) [17, 18], a 1:1 relative occupation has been assumed. One exception is a diffuse LEED study [53] of low-coverage NO on Ni(111) (also at an approximate coverage of 0.25 ML), but in this case the structural parameters of the NO molecules in each site were not allowed to be optimized at each composition as we have done here. Indeed, the mixture of sites used was based on a best-fit pure fcc site occupation local structure, and a best-fit pure hcp site occupation local structure. The

two local structures had N–Ni nearest-neighbour distances which differed by 0.39 Å which seems clearly unphysical, leaving the results subject to considerable doubt. It is perhaps worth remarking that a conventional LEED study of either the Ni(111)(2 × 2)-CO phase, or the Ni(100)c(2 × 2)-CO phase at different temperatures could be of considerable interest. Both PhD and vibrational spectroscopy provide information which is local in character, whereas conventional LEED selectively samples the long-range-order components. LEED would therefore be ‘blind’ to the second site in these systems if it was a consequence of local disorder, but would produce an incoherent sum of the two structures if ordered domains of each are involved; as such, the combined studies could clarify the true long-range structure of these systems.

In summary, therefore, our main conclusion is that while CO on Ni(111) does appear to show a marginal preference for occupation of hcp hollow sites over fcc hollow sites, there is no significant difference in the relative site occupation between the 0.5 ML c(4 × 2) phase and a 0.25 ML phase which shows a (2 × 2) LEED pattern. A perfect single-domain long-range-ordered 0.25 ML (2 × 2) phase cannot be reconciled with more than a single adsorption site, and we conclude that for this surface at least, either the surface must show considerable disorder (which may be within regions of average (2 × 2) periodicity or in truly disordered regions, or both), or must comprise a two-domain structure with each domain being based on one of the two hollow sites. Furthermore, we conclude that the occupation of the two hollow sites in the c(4 × 2) phase cannot be attributed solely to nearest-neighbour adsorbate–adsorbate repulsions, but rather that the two local sites differ in binding energy by too small an amount for a condensation to occur into a single site at temperatures above 115 K.

Acknowledgments

The authors are pleased to acknowledge the financial support of this work in the form of grants from the Engineering and Physical Science Research Council (UK), the European Community through the Human Capital and Mobility Networks (grant No ERBCHRXCT930358) and Large Scale Facilities programmes, and the German Federal Ministry of Education, Science, Research and Technology (BMBF) under contract number 05 625EBA 6.

References

- [1] Schindler K M, Hofmann P, Weiss K-U, Dippel R, Gardner P, Fritzsche V, Bradshaw A M, Woodruff D P, Davila M E, Asensio M C, Conesa J C and González-Elipe A R 1993 *J. Electron. Spectrosc. Relat. Phenom.* **64/65** 75
- [2] Davila M E, Asensio M C, Woodruff D P, Schindler K M, Hofmann P, Weiss K U, Dippel R, Gardner P, Fritzsche V, Bradshaw A M, Conesa J C and González-Elipe A R 1994 *Surf. Sci.* **311** 337
- [3] Becker L, Aminpirooz S, Hillert B, Pedio M, Haase J and Adams D L 1993 *Phys. Rev. B* **47** 9710
- [4] Bertolini J C, Dalmai-Imelik G and Rousseau J 1977 *Surf. Sci.* **68** 539
- [5] Erley W, Wagner H and Ibach H 1979 *Surf. Sci.* **80** 612
- [6] Campuzano J C and Greenler R G 1979 *Surf. Sci.* **83** 301
- [7] Bertolini J C and Tardy B 1981 *Surf. Sci.* **102** 131
- [8] Trenary M, Uram K J and Yates J T Jr 1985 *Surf. Sci.* **157** 512
- [9] Trenary M, Uram K J, Bozso F and Yates J T Jr 1984 *Surf. Sci.* **146** 269
- [10] Persson B N J and Ryberg R 1985 *Phys. Rev. Lett.* **54** 2119
- [11] Tang S L, Lee M B, Yang O Y, Beckerle Y D and Ceyer C T 1986 *J. Chem. Phys.* **84** 1876
- [12] Surnev L, Xu Z and Yates J T Jr 1988 *Surf. Sci.* **201** 1, 14
- [13] Chen J G, Erley W and Ibach H 1989 *Surf. Sci.* **223** L891

- [14] Mapledoram L D, Bessent M P, Wander A and King D A 1994 *Chem. Phys. Lett.* **228** 527
- [15] Watson P R, Van Hove M A and Hermann K 1993 *NIST Surface Structure Database—Version 1* National Institute of Standards and Technology, Gaithersburg, MD
- [16] Kerker M, Hayden A B, Woodruff D P, Kadodwala M and Jones R G 1992 *J. Phys.: Condens. Matter* **4** 5043
- [17] Farrell H H, Traum M M, Smith N V, Woodruff D P and Johnson P D 1981 *Surf. Sci.* **102** 527
- [18] Kang W M, Li C H and Tong S Y 1980 *Solid State Commun.* **36** 149
- [19] Grimsby D T, Wu Y K and Mitchell K A R 1990 *Surf. Sci.* **252** 51
Schmidtke E, Schwennicke C and Pfnur H 1994 *Surf. Sci.* **312** 301
- [20] Mendez M A, Oed W, Fricke L, Hammer L, Heinz K and Müller K 1991 *Surf. Sci.* **253** 99
- [21] Kortan A R and Park R L 1981 *Phys. Rev. B* **23** 6340
- [22] Woodruff D P and Bradshaw A M 1994 *Rep. Prog. Phys.* **57** 1029
- [23] Bradshaw A M and Woodruff D P 1995 *Applications of Synchrotron Radiation: High-Resolution Studies of Molecules and Molecular Adsorbates on Surfaces* ed W Eberhardt (Berlin: Springer) p 127
- [24] Fernandez V, Schindler K M, Schaff O, Hofmann P, Theobald A, Bradshaw A M, Fritzsche V, Davis R and Woodruff D P 1996 *Surf. Sci.* at press
- [25] Davis R, Woodruff D P, Schaff O, Fernandez V, Schindler K M, Hofmann P, Weiss K-U, Dippel R, Fritzsche V and Bradshaw A M 1995 *Phys. Rev. Lett.* **74** 1621
- [26] Davis R, Woodruff D P, Schaff O, Fernandez V, Schindler K M, Hofmann P, Weiss K-U, Dippel R, Fritzsche V and Bradshaw A M 1996 to be published
- [27] Dietz E, Braun W, Bradshaw A M and Johnson R L 1985 *Nucl. Instrum. Methods A* **239** 359
- [28] Germer L H, Scheibner E J and Hartman C D 1960 *Phil. Mag.* **5** 222
- [29] Edmonds T and Pitkethly R C 1969 *Surf. Sci.* **15** 137
- [30] Christmann K, Schober O and Ertl G 1974 *J. Chem. Phys.* **60** 4719
- [31] Conrad H, Ertl G, Kuppers J and Latta E E 1976 *Surf. Sci.* **57** 475
- [32] Erley W, Besocke K and Wagner H 1974 *J. Chem. Phys.* **66** 5269
- [33] Kevan S D, Davies R F, Rosenblatt D H, Tobin J G, Mason M G, Shirley D A, Li C H and Tong S Y 1981 *Phys. Rev. Lett.* **46** 1629
- [34] Hofmann P, K-M. Schindler, Bao S, Fritzsche V, Ricken D E, Bradshaw A M, and Woodruff D P 1994 *Surf. Sci.* **304** 74
- [35] Fritzsche V and Woodruff D P 1992 *Phys. Rev. B* **46** 16128
- [36] Schindler K M, Hofmann P, Fritzsche V, Bao S, Kulkarni S, Bradshaw A M and Woodruff D P 1993 *Phys. Rev. Lett.* **71** 2054
- [37] Hofmann P, K-M. Schindler, Fritzsche V, Bao S, Bradshaw A M and Woodruff D P 1994 *J. Vac. Sci. Technol. A* **12** 2045
- [38] Hofmann P and Schindler K M 1993 *Phys. Rev. B* **47** 13942
- [39] Hofmann P, Schindler K M, Bao S, Bradshaw A M and Woodruff D P 1994 *Nature* **368** 131
- [40] Fritzsche V 1990 *J. Phys.: Condens. Matter* **2** 9735
- [41] Fritzsche V 1992 *J. Electron. Spectrosc. Relat. Phenom.* **58** 299
- [42] Fritzsche V 1992 *Surf. Sci.* **265** 187
- [43] Fritzsche V and Pendry J B 1993 *Phys. Rev. B* **48** 9054
- [44] Dippel R, Weiss K U, Schindler K M, Gardner P, Fritzsche V, Bradshaw A M, Asensio M C, Hu X M, Woodruff D P and González-Elipe A R 1992 *Chem. Phys. Lett.* **199** 625
- [45] Pendry J B 1980 *J. Phys. C: Solid State Phys.* **13** 937
- [46] Lauterbach J, Wittmann M and Kuppers J 1992 *Surf. Sci.* **279** 287
- [47] Yoshinobu J and Kawai M 1993 *Chem. Phys. Lett.* **211** 48
- [48] Yoshinobu J, Takagi N and Kawai M 1993 *J. Electron. Spectrosc. Relat. Phenom.* **64/65** 207
- [49] Grossmann A, Erley W and Ibach H 1993 *Phys. Rev. Lett.* **71** 2078
- [50] Martin R, Gardner P and Bradshaw A M 1995 *Surf. Sci.* **342** 69
- [51] Andersson S and Pendry J B 1979 *Phys. Rev. Lett.* **43** 363; 1980 *J. Phys. C: Solid State Phys.* **13** 3547
- [52] Tong S Y, Maldonado A, Li C H and Van Hove M A 1980 *Surf. Sci.* **94** 73
- [53] Mapledoram L D, Wander A and King D A 1994 *Surf. Sci.* **312** 54